Exploring Mechanism of Generating Spin-Orbital Coupling through Donor-Acceptor Design to Realize Spin Flipping in Thermally Activated Delayed Fluorescence

Exploring Mechanism of Generating Spin-Orbital Coupling through Donor-Acceptor Design to Realize Spin Flipping in Thermally Activated Delayed Fluorescence

Miaosheng Wang[a], Tanmay Chatterjee[b], Camera Janelle Foster[a], Ting Wu[a], Chih-Lun Yi[b], Haomiao Yu[c], Ken-Tsung Wong[b,*] and Bin Hu[a,*]

[a] *Joint Institute for Advanced Materials, Department of Materials Science and Engineering, University of Tennessee, Knoxville, TN 37996, USA*

[b] *Department of Chemistry, National Taiwan University, and Institute of Atomic and Molecular Science Academia Sinica, Taipei 10617, Taiwan*

[c] *Key Laboratory of Luminescence and Optical Information, Ministry of Education, School of Science, Beijing Jiaotong University, Beijing 100044, China*

*Corresponding authors:

Ken-Tsung Wong: Email: kenwong@ntu.edu.tw

Bin Hu, E-mail: bhu@utk.edu

30 **Abstract**

31   Spin flipping has been recently recognized as the critical mechanism to enable the conversion

32   from non-radiative triplets into radiative singlets, leading to thermally assisted delayed

33   fluorescence (TADF) in organic light-emitting diodes (OLEDs). However, it is a controversial

34   issue on how spin flipping is realized in the absence of heavy elements. This paper reports clear

35   evidence to show that spin-orbital coupling (SOC) is indeed formed in charge-transfer (CT)

36   states through donor-acceptor (D-A) design by using magneto-photoluminescence (magneto-

37   PL), in both steady and dynamic states. Essentially, a magneto-PL signal is observed at high

38   field (up to 900 mT) only if CT states are excited within D-A structures in a typical TADF

39   emitter DMAC-TRZ in solutions. This presents unambiguous evidence to show the existence

40   of SOC in TADF molecules where heavy elements are absent. The empirical model is proposed

41   to show the SOC generated in CT states by considering orbital polarizations by optically

42   induced dipoles ($D^+ \rightarrow A^-$). Furthermore, SOC is confirmed to be responsible for realizing spin

43   flipping by directly monitoring the delayed fluorescence while the density of non-radiative

44   triplets is changed by oxygen molecules. More importantly, by using solvent polarity to change

45   the dipole moment in CT states, it is revealed that SOC-induced spin flipping is largely changed,

46   presenting a unified relationship between SOC and dipole moment to control the spin flipping

47   to enable the conversion from non-radiative triplets into radiative singlets in TADF.

48

49

50

Introduction

The success of thermally activated delayed fluorescence (TADF) provides an excellent example to indicate that spin-flipping functions as the necessary condition to harvest non-radiative triplets into radiative singlets towards developing high external quantum efficiency (EQE) in organic light-emitting diodes (OLEDs).[1,2,3,4,5,6,7] The experimental studies have indicated that the spin flipping is largely enhanced upon decreasing the singlet-triplet energy difference (ΔE_{ST}) in TADF molecules.[8,9] The recent studies directly observed the intersystem crossing from triplets to singlets in TADF molecules by monitoring exciton dynamics upon PL quenching.[10] Therefore, there must exist a mechanism to effectively flip the spins of triplets to enable the reverse intersystem crossing (rISC) into light-emitting singlets in TADF molecules. Based on the success of 2nd generation of phosphorescence organic emitters where spin-orbital coupling (SOC) functions as an efficient mechanism to flip the spins of triplet excitons upon using heavy elements, we can expect that TADF molecules possess a strong SOC to enable the spin-flipping to harvest triplet excitons. There are several factors that can initiate SOC in organic materials such as heavy element effects, aromatic carbonyls, and hydron bonding.[11] Among these factors, the heavy element effect is the most efficient one to generate SOC and consequently harvest triplet states through the phosphorescence process in organic light-emitting materials. However, the experimental investigations on SOC effects in organic TADF emitters with only light elements are still in urgent needs.

It is generally believed that decreasing the ΔE_{ST} is an essential approach to facilitate the conversion from non-radiative triplet states to singlet states for generating an efficient TADF. However, the opposite examples of poor TADF compounds with very small ΔE_{ST} and very efficient TADF compounds with large ΔE_{ST} of few hundreds meV have indicated that energy splitting is not the only determining parameter in TADF system.[12,13,14,15] Indeed, the ΔE_{ST}-dependent rISC can be validated to generate TADF only if SOC is existed to induce spin flipping of triplet excitons.[16] When the SOC is established as the spin flipping mechanism, the spin mixing between singlets and triplets can be then controlled by the energy parameter. Generally, the spin mixing rate (λ) can be expressed as $\lambda = H_{SO}/\Delta E_{ST}$, where H_{SO} and ΔE_{ST} are the SOC constant and energy difference between S_1 and T_1 states.[17] Therefore, the spin flipping is the precondition to validate the ΔE_{ST}-dependent rISC. However, it has been remained as an un-raveled issue to experimentally address SOC effects responsible for operating high-efficiency TADF. Further intriguingly, after spin flipping, the triplet states must undergo an endothermic process via thermal energy to reach the light-emitting singlets states towards

84   generating a high-efficiency TADF rather than to exothermically relax to ground state (S_0) for

85   a low-efficiency phosphorescence. This requires an electric-magnetic coupling between

86   singlets and the triplets to enable the rISC towards TADF by preventing the triplet-to-S_0

87   phosphorescence. In this work, we utilized magneto-PL in both steady and time-resolved

88   regimes to explore the underlying spin-dependent processes of enabling high-efficiency TADF.

89

90   **Results and Discussions**

91   Here, the magneto-EL is used to show the existence of SOC as the dominant spin-

92   flipping mechanism in TADF process by comparing the highly efficient TADF emitter DMAC-

93   TRZ [18] with the traditional fluorescence organic emitter poly(p-phenylene vinylene) (MEH-

94   PPV). The EL spectra of the DMAC-TRZ and MEH-PPV based OLEDs are shown in Figure

95   1a. Then we measured the magneto-EL for both OLEDs under constant current mode. We must

96   note that magnetic field effects can occur in hyperfine interaction (HFI) (< 10 mT) or SOC (>

97   10 mT) regimes when an external magnetic field competes with HFI or SOC to change the

98   singlet and triplet populations, generating the so-called spin-mixing between singlet and triplet

99   states. When the SOC is absent and the HFI governs the spin-mixing, magnetic field effects

100   are always occurred at low field (< 10 mT).[19,20,21] Indeed, in MEH-PPV OLED with negligible

101   SOC, the internal magnetic parameter (B_0) of the magneto-EL curve is in the HFI regime (6.4

102   mT), as shown in Figure 1b. When the SOC exists, magnetic field effects can be observed at

103   high field and the width of the curves becomes significantly broader as compared with HFI

104   condition.[22,23,24] Therefore, the high field magnetic field effect signals can serve as evidence to

105   indicate that the SOC is formed to function as the dominating mechanism for spin-flipping in

106   organic systems.[25,26,27] Interestingly, we observed magneto-EL in DMAC-TRZ based OLED

107   in high field with much broader curve shape (B_0=70.5 mT), as compared with MEH-PPV based

108   OLED in HFI regime with narrow curve shape. Clearly, this high field magneto-EL in DMAC-

109   TRZ based OLED provides direct evidence to show the existence of SOC as the dominant spin-

110   flipping mechanism in TADF process.

111   Then we used magneto-PL to illuminate how the SOC is formed to initiate the spin

112   mixing towards TADF process based on DMAC-TRZ molecule in solutions. The molecular

113   structure of the TADF emitter DMAC-TRZ used in this work is shown as the inset in Figure

114   2a. Figure 2a shows the UV-Vis absorption spectrum of DMAC-TRZ in toluene solution. The

115   strong absorption of DMAC-TRZ at around 300 nm belongs to the π-π* excitonic transition,

116   while the broad absorption peak at 386 nm is attributed to the intramolecular CT states. The

117   DMAC-TRZ molecule contains donor-acceptor structure within a π-conjugated system. As a

118   result, both excitonic and CT states co-exist within close proximity. Figure 2b shows the PL

119   spectra from DMAC-TRZ toluene solution under 325 nm, 375 nm and 405 nm continuous

120   wave (CW) laser excitations. The same light-emitting states (^{1}CT) in DMAC-TRZ molecule

121   are generated under different photoexcitation wavelengths, as indicated by the similar PL

122   spectra. Figure 2c shows interesting magneto-PL behaviors of DMAC-TRZ in toluene solution

123   at different excitation wavelengths (325 nm, 375 nm, and 405 nm) from the laser beams. The

124   magneto-PL signals were observed at the magnetic field much larger than the HFI field strength,

125   confirming that the SOC is indeed formed in this TADF-based molecule. Moreover, it is very

126   interesting to note that this high-field magneto-PL can be observed only if the CT states are

127   excited. For example, exciting CT states by using the photoexcitation at 405 nm and 375 nm

128   generates an appreciable magneto-PL signal at high field with the B_0 of 224 mT. This reveals

129   that the SOC occurs in CT states. In contrast, exciting the excitonic states by using 325 nm

130   laser beam leads to a negligible magneto-PL signal, indicating that the SOC is lacking in

131   excitonic states. We should note that, by using short-wavelength excitation to excite localized

132   excitonic states, the CT states can be also formed through charge separation. However, the

133   efficiency of generating CT states through localized states separation is much lower than

134   directly exciting CT states with long-wavelength excitation, as shown in the excitation

135   spectrum in Figure S1. Therefore, short-wavelength and long-wavelength excitations can

136   generate low and high densities of CT states, respectively. Clearly, our magneto-PL results

137   show that exciting CT and excitonic states lead to appreciable and negligible SOC in DMAC-

138   TRZ molecules. Note that the concentration of the DMAC-TRZ does not have a significant

139   influence on the magneto-PL signals (Figure S2). To confirm that high-field magneto-PL can

140   represent the SOC, we have further measured the magneto-PL from light-emitting CT states

141   formed by physically mixing *N,N′*-bis(3-methylphenyl)-*N,N′*-diphenylbenzidine (TPD) and

142   2,5-bis-(5-tert-butyl-2-benzoxazolyl)thiophene (BBOT) in toluene solution. Here, we can see

143   that the light-emitting CT states in physically mixed TPD:BBOT solution still shows a

144   magneto-PL at high field (> 10 mT) (Figure S3). Because of negligible exchange interaction

145   due to large separation distance between the TPD and BBOT molecules in the liquid state,

146   magneto-PL is solely governed by SOC through spin mixing. Thus, this high-field magneto-

147   PL serves as direct evidence to show the existence of SOC in CT states. To examine our

148   observation is not limited only to DMAC-TRZ, we adopted the same protocol on two additional

149   molecules DMAC-PymCN and DMAC-PmmCN with weaker and stronger TADF properties,

150   respectively, as shown in Figure S4. It can be seen that DMAC-PymCN and DMAC-PmmCN

151   molecules give smaller and larger magneto-PL signals, corresponds to weaker and stronger

152   spin-mixing, respectively. More importantly, both TADF molecules demonstrate magneto-PL

153   signals at high field regime (>10 mT). This information is in good consistent with the high-

154   field magneto-PL signals observed in DMAC-TRZ molecule, indicating the SOC as the spin-

155   flipping mechanism in TADF molecules designed with donor-acceptor structure.

156   Here, the observed magneto-PL signals in organic TADF molecule indicate that there

157   must exist a mechanism to generate SOC by using CT states. Here, we consider that photo-

158   induced charge transfer between the donor (D) and acceptor (A) leads to positively and

159   negatively charged moieties (D^+ and A^-) in a CT state, giving an optically induced dipole

160    $D^+ \rightarrow A^-$. Before exciting CT states, the D and A have negligible SOC due to isotropically

161   distributed orbitals. We propose that the isotropically distributed orbitals are asymmetrically

162   polarized by the optically induced dipole $D^+ \rightarrow A^-$ in CT states. Consequently, asymmetrically

163   polarized orbitals interact with spins on D^+ and A^-, generating SOC within CT states, as

164   schematically illustrated in Figure 2d. This proposed scenario can be supported by our previous

165   studies, where we found that an optically excited CT state can directly interact with

166   ferromagnetic nanoparticle, leading to magnetic field effects in the SOC regime (> 10 mT).[28,29]

167   This observation indicates that the interaction between an electric dipole and a spin dipole can

168   be equivalently considered as SOC. Clearly, the SOC formed in the CT states of a TADF-based

169   molecule provides the necessary mechanism to flip the spins to enable the TADF.

170   Then, we investigated the SOC-enabled spin flipping to generate TADF through rISC

171   process. In general, there are three possibilities for spin-mixing to occur within excitonic states

172   (between ^1LE and ^3LE), within CT states (between ^1CT and ^3CT), and between excitonic and

173   CT states (^3LE to ^1CT). It should be noted that both excitonic and intramolecular CT states

174   have a strong exchange interaction due to short electron-hole distance. A strong exchange

175   interaction can largely enhance the spin-conservation behavior, minimizing intersystem

176   crossing between singlet and triplet states.[30,31] This leads to the only possibility that the

177   intersystem crossing occurs between CT and excitonic states in TADF molecules. Here, we

178   simultaneously monitored the spin-mixing and delayed fluorescence while the density of triplet

179   excitons is changed by using O_2 gas. Using O_2 is a practical method to quench the excited states

180   in solutions. [32,33] In principle, the O_2 can react with both excitons and CT states. However, in

181   excitonic states, the O_2 can more selectively react with ^3LE due to largely different lifetime and

182   ionic properties between ^1LE and ^3LE. In CT states, the O_2 can react with both ^1CT and ^3CT

183   because of similar lifetime and ionic properties between ^{1}CT and ^{3}CT. Therefore, using the O_2

184   can confirm the spin flipping occurring in triplet excitons while monitoring magneto-PL. It can

185   be seen in Figure 3a that the delayed fluorescence intensity is largely decreased upon

186   introducing O_2 molecules. The PL quenching shown in Figure 3b provides a further indication

187   that introducing O_2 molecules can decrease the density of triplet excitons with the consequence

188   of quenching the delayed fluorescence. Concurrently, the spin-mixing disappeared, shown as

189   a negligible magneto-PL signal (Figure 3c). In contrast, magneto-PL signal is preserved under

190   N_2 condition, indicating that the spin-mixing evidently occurs when the triplet excitons are

191   maintained. The simultaneous occurrence of spin-mixing and delayed fluorescence provides

192   direct evidence to support that the SOC flips the spins of triplet excitons to generate a TADF

193   through rISC. The early publications have proposed that the ^{3}LE state can reach an equilibrium

194   with the ^{3}CT state through spin-conserving process and followed by a spin-mixing from ^{3}LE

195   to ^{1}CT to generate a TADF.[34,35,36] In our studies, we can see that the spin-mixing does not occur

196   in intramolecular CT states (between ^{1}CT and ^{3}CT) because the magneto-PL signal, used to

197   show spin-mixing, disappeared when the ^{3}LE states are quenched by the O_2 molecules (Figure

198   3c). The absence of spin-mixing in intramolecular CT states implies that the CT states have a

199   strong exchange interaction due to the short D-A distance to prevent the ^{3}CT to ^{1}CT conversion.

200   We should note that the absence of spin-mixing in CT states does not cause a loss of the TADF

201   since the ^{3}CT states can convert into ^{3}LE states through spin-conserving process. When the

202   SOC in CT states flips the spins of ^{3}LE state, then spin-mixing occurs from ^{3}LE state to ^{1}CT

203   state towards generating a TADF. This is confirmed by comparing the PL decay curves

204   measured under zero field and magnetic field of 200 mT, in which the time-resolved magneto-

205   PL can be extracted. Figure 4a shows that in nitrogen condition with the presence of high field

206   of 200mT, the PL change gradually increases with decay time, reaching 20% at 102 ns. When

207   the delayed fluorescence is largely reduced by using O_2 molecules to quench the triplet excitons,

208   the PL lifetime becomes insensitive to the magnetic field within the entire time window up to

209   5 μs (Figure 4b). Clearly, the results obtained from time-resolved magneto-PL confirm that the

210   SOC in the CT states flips the spins of ^{3}LE state, generating a spin-mixing to convert the ^{3}LE

211   state into ^{1}CT state towards TADF.

212   The solvent polarity effects are used to further test the SOC required to allow the spin-

213   mixing between ^{1}CT and ^{3}LE. The polarity of the environment can change the dipole moment

214   and the energy level of CT states while leaving the LE states almost unaffected, leading to

215   solvatochromism effects. [35,37] Here, we use magneto-PL to monitor the spin-mixing while the

216   dipole moment and energy level of the CT states is changed by increasing the solvent polarity.

217   As shown in Figure 5a, increasing the solvent polarity from hexane (relative polarity 0.009) to

218   p-xylene (relative polarity: 0.077), and toluene (relative polarity: 0.099) leads to a red-shift on

219   the PL spectrum with the peak wavelength changing from 441 nm to 489 nm and 495 nm,

220   respectively. Clearly, increasing the solvent polarity can down-shift the energy of CT states

221   towards the local excitonic states, increasing the delayed fluorescence component (Figure 5b

222   and 5c). Simultaneously, we can see in Figure 5d that the spin-mixing is largely increased as

223   the solvent polarity is increased, as shown by the increased magneto-PL in high field SOC

224   regime. Furthermore, it can be seen that with further increased solvent polarity in

225   chlorobenzene solution (relative polarity 0.188), both TADF efficiency and magneto-PL signal

226   are reduced as compared with the toluene solution condition because CT states move out of

227   resonance with the LE states. Clearly, this magneto-PL result provides a direct experimental

228   confirmation to show that the spin-mixing is increased through SOC-enabled spin flipping as

229   the energy difference between ^{1}CT state and excitonic state (^{3}LE) is decreased in TADF

230   molecules.

231   Here we discuss the electric magnetic coupling between ^{1}CT and ^{3}LE to enable the

232   spin-dependent TADF. Our magneto-PL studies indicate that the spin-mixing is occurring from

233   ^{3}LE state to ^{1}CT state when the SOC in CT states flips the spins of triplet excitons, as illustrated

234   in Figure 6. It should be pointed out that triplet excitons can generate two outcomes after spin

235   flipping by SOC: (i) a delayed fluorescence through endothermic rISC process from ^{3}LE state

236   to ^{1}CT state; (ii) a phosphorescence through exothermic process from ^{3}LE state to ground state

237   (^{0}S). The experimental observation of delayed fluorescence implies that there must be an

238   attractive interaction between ^{1}CT and ^{3}LE states to enforce the endothermic process from ^{3}LE

239   state to ^{1}CT state towards generating delayed fluorescence. Essentially, this attractive

240   interaction together with thermal energy can enable the conversion from ^{3}LE state to ^{1}CT state

241   through an endothermic process which generates delayed fluorescence by preventing the ^{3}LE

242   state relaxing to ground state after the SOC flips the spins of ^{3}LE state. Therefore, the

243   contribution of phosphorescence to the total emission in TADF process is negligible especially

244   at room temperature. It is noted that the vibronic coupling has been proposed to explain the

245   coupling between ^{3}LE and ^{3}CT states based on the observation where the TADF is a function

246   of host polarity.[35,36, 38,39] Here we consider an electric-magnetic coupling between ^{1}CT and ^{3}LE

247   states as the necessary condition to enable the ^{3}LE $\rightarrow^1$CT intersystem crossing. The electric-

248   magnetic coupling can occur with very weak spins such as paramagnetic materials when placed

249   within close proximity with electrical dipoles.[40,41] And triplet excitons can be regarded as

250   paramagnetic.[42] Furthermore, we found that an electric-magnetic coupling can indeed exist

251   between an electric dipole and a spin dipole located within close proximity in

252   ferromagnetic/organic composites.[28,29,43] In TADF systems, ^{1}CT and ^{3}LE states are equivalent

253   to electric and spin dipoles, respectively. Therefore, we expect an electric-magnetic coupling

254   between ^{1}CT and ^{3}LE states enables the endothermic ^{3}LE $\rightarrow$^{1}CT intersystem crossing towards

255   TADF, when the energy conversation requirement is satisfied by using thermal energy. The

256   electric-magnetic coupling can occur through three possible channels: 1) long-range Coulomb

257   interaction; 2) midrange spin-orbital coupling interaction; 3) short-range spin-spin interaction,

258   between an electric dipole and a spin. Even though it is still unclear on the contributions for

259   each channel, the electric-magnetic coupling between ^{3}LE and ^{1}CT serves as an important

260   parameter accountable for both spin flipping of ^{3}LE and realizing the endothermic spin-mixing

261   from ^{3}LE to ^{1}CT to generate a high-efficiency TADF.

262   The electric-magnetic coupling between ^{3}LE and ^{1}CT states allows the conversion from

263   ^{3}LE state to ^{1}CT state, in which the spin-mixing process is accountable for TADF after the

264   SOC in CT states flips the spins of ^{3}LE state. For a high-efficiency TADF, the ^{1}LE and ^{3}CT

265   states must be converted into the light-emitting ^{1}CT state to avoid a loss in excited states. The

266   ^{1}LE state can directly relax to light-emitting ^{1}CT state through a spin-conserving process,

267   according to the PL generated from CT states by exciting excitonic states. Similarly, the ^{3}CT

268   states can relax to ^{3}LE states under spin conservation followed by the spin-mixing towards

269   light-emitting ^{1}CT state. Therefore, both ^{1}LE and ^{3}CT states can effectively be converted to the

270   light-emitting ^{1}CT state. We should further note that there is a possibility that the ^{3}LE state

271   may be converted to ^{3}CT state under thermal activation through spin-conserving process. If

272   this occurs, it would generate a loss in TADF since the strong exchange interaction does not

273   allow the ^{3}CT$\rightarrow$^{1}CT conversion. However, this possibility can be eliminated because the spin-

274   mixing from ^{3}LE state to ^{1}CT state can shorten the lifetime of ^{3}LE state as compared to the rate

275   of ^{3}LE$\nrightarrow$^{3}CT conversion, consequently suppressing the backward conversion from ^{3}LE state

276   to ^{3}CT state and enhancing the forward conversion from ^{3}CT state to ^{3}LE state to avoid any

277   loss in TADF.

278

Conclusions

280   In summary, we found that the TADF molecule (DMAC-TRZ) based OLEDs

281   demonstrated a magneto-EL in high field regime (> 10 mT). This high-field magneto-EL signal

282   provides direct evidence to indicate that the SOC is indeed formed, in the absence of heavy

283 elements, towards developing the spin-dependent TADF in OLEDs. This finding brings two
284 open questions: where is SOC formed and how does SOC enable the spin-mixing towards
285 generating TADF? By using magneto-PL to explore the origin of SOC, we observed that
286 exciting CT states can lead to a magneto-PL signal in SOC regime (high field > 10 mT) with a
287 delayed fluorescence while exciting local excitonic states does not generate any detectable
288 magneto-PL signal. This observation provides the first experimental indication that the SOC is
289 formed in CT states. We propose that an optically induced electrical dipole between D^+ and A^-
290 can partially polarize the orbitals on D^+ and A^-, and consequently generates a strong SOC
291 within a CT state. To understand the spin-mixing in developing the TADF, we found that
292 decreasing the density of triplet excitons (^{3}LE) by using O_2 can largely decrease the delayed
293 fluorescence and magneto-PL signal, both in steady-state and transient measurements. This
294 result indicates that the SOC in CT states flips the spins of ^{3}LE state to enable the spin-mixing
295 from ^{3}LE state to ^{1}CT state towards TADF. Furthermore, the spin-mixing from ^{3}LE state to
296 ^{1}CT state requires an attractive interaction between ^{3}LE and ^{1}CT states to enable this
297 endothermic process towards delayed fluorescence by avoiding the exothermic spin-mixing
298 from ^{3}LE state to ^{0}S state towards phosphorescence. We consider the electric-magnetic
299 coupling between ^{1}CT and ^{3}LE states as the underlying mechanism to enable the endothermic
300 intersystem crossing (^{3}LE $\rightarrow$ ^{1}CT) which in turn generates a high-efficiency TADF. Clearly,
301 our magneto-PL studies provide an insightful understanding on the SOC effects of spin-mixing
302 towards generating TADF. We believe that the results disclosed in this work can shed light on
303 the detailed mechanisms involved in TADF with intramolecular CT features and can trigger
304 new ideas for creating more efficient molecules towards practical applications in OLEDs.

305

306 **Conflicts of interest**

307 There are no conflicts of interest to declare.

308 **Acknowledgments**

318

319   **References**

_____

[1] H. Tanaka, K. Shizu, H. Miyazaki and C. Adachi, *ChemCommun*, 2012, **48**, 11392-11394.

[2] A. Endo, M. Ogasawara, A. Takahashi, D. Yokoyama, Y. Kato and C. Adachi, *Adv. Mater.*, 2009, **21**, 4802-4806.

[3] H. Uoyama, K. Goushi, K. Shizu, H. Nomura and C. Adachi, *Nature*, 2012, **492**, 234.

[4] H. Wang, L. Xie, Q. Peng, L. Meng, Y. Wang, Y. Yi and P. Wang, *Adv. Mater.*, 2014, **26**, 5198-5204.

[5] B. S. Kim and J. Y. Lee, *Adv. Funct. Mater.*, 2014, **24**, 3970-3977.

[6] D. R. Lee, M. Kim, S. K. Jeon, S. H. Hwang, C. W. Lee and J. Y. Lee, *Adv. Mater.*, 2015, **27**, 5861-5867.

[7] Y. Liu, C. Li, Z. Ren, S. Yan and M. R. Bryce, *Nat. Rev. Mater.*, 2018, **3**, 18020.

[8] K. Goushi, K. Yoshida, K. Sato and C. Adachi, *Nat. Photonics*, 2012, **6**, 253.

[9] P. L. Santos, J. S. Ward, P. Data, A. S. Batsanov, M. R. Bryce, F. B. Dias and A. P. Monkman, *J. Mater. Chem.*, 2016, **4**, 3815-3824.

[10] B. Yurash, H. Nakanotani, Y. Olivier, D. Beljonne, C. Adachi and T.-Q. Nguyen, *Adv. Mater.*, 2019,1804490.

[11] O. Bolton, K. Lee, H.-J. Kim, K. Y. Lin and J. Kim, *Nat. Chem.*, 2011, **3**, 205.

[12] N. Haase, A. Danos, C. Pflumm, A. Morherr, P. Stachelek, A. Mekic, W. Brütting and A. P. Monkman, *J. Phys. Chem. C*, 2018, **122**, 29173-29179.

[13] D. Zhang, M. Cai, Y. Zhang, D. Zhang and L. Duan, *Mater. Horiz.*, 2016, **3**, 145-151.

[14] T. Hosokai, H. Matsuzaki, H. Nakanotani, K. Tokumaru, T. Tsutsui, A. Furube, K. Nasu, H. Nomura, M. Yahiro and C. Adachi, *Sci. Adv.*, 2017, **3**, e1603282.

[15] F. B. Dias, K. N. Bourdakos, V. Jankus, K. C. Moss, K. T. Kamtekar, V. Bhalla, J. Santos, M. R. Bryce and A. P. Monkman, *Adv. Mater.*, 2013, **25**, 3707-3714.

[16] Y. Olivier, B. Yurash, L. Muccioli, G. D'Avino, O. Mikhnenko, J.-C. Sancho-Garcia, C. Adachi, T.-Q. Nguyen and D. Beljonne, *Phys. Rev. Mater.*, 2017, **1**, 075602.

[17] H. Noda, X.-K. Chen, H. Nakanotani, T. Hosokai, M. Miyajima, N. Notsuka, Y. Kashima, J.-L. Brédas and C. Adachi, *Nat. Mater.*, 2019, 1-7.

[18] W.-L. Tsai, M.-H. Huang, W.-K. Lee, Y.-J. Hsu, K.-C. Pan, Y.-H. Huang, H.-C. Ting, M. Sarma, Y.-Y. Ho, H.-C. Hu, K.-T. Wong and C.-C. Wu, *ChemCommun*, 2015, **51**, 13662-13665.

[19] T. D. Nguyen, G. Hukic-Markosian, F. Wang, L. Wojcik, X.-G. Li, E. Ehrenfreund and Z. V. Vardeny, *Nat. Mater.*, 2010, **9**, 345.

[20] P. Bobbert, T. Nguyen, F. Van Oost, v. B. Koopmans and M. Wohlgenannt, *Phys. Rev. Lett.*, 2007, **99**, 216801.

[21] Z. Yu, F. Ding and H. Wang, *Phys. Rev. B*, 2013, **87**, 205446.

[22] Y. Sheng, T. Nguyen, G. Veeraraghavan, Ö. Mermer and M. Wohlgenannt, *Phys. Rev. B*, 2007, **75**, 035202.

[23] T. D. Nguyen, Y. Sheng, J. Rybicki, G. Veeraraghavan and M. Wohlgenannt, *J. Mater. Chem.*, 2007, **17**, 1995-2001.

[24] J. Rybicki, T. D. Nguyen, Y. Sheng and M. Wohlgenannt, *Synth. Met.*, 2010, **160**, 280-284.

[25] M. Wang, Y. H. Huang, K. S. Lin, T. H. Yeh, J. Duan, T. Y. Ko, S. W. Liu, K. T. Wong and B. Hu, *Adv. Mater.*, 2019, 1904114.

[26] R. Geng, T. T. Daugherty, K. Do, H. M. Luong and T. D. Nguyen, *J. Sci. Adv. Mater. Devices*, 2016, **1**, 128-140.

[27] S. Liang, R. Geng, B. Yang, W. Zhao, R. C. Subedi, X. Li, X. Han and T. D. Nguyen, *Sci. Rep.*, 2016, **6**, 19461.

[28] M. Li, M. Wang, L. He, Y. C. Hsiao, Q. Liu, H. Xu, T. Wu, L. Yan, L. S. Tan and A. Urbas, *Adv. Electron. Mater.*, 2015, **1**, 1500058.

[29] L. Yan, M. Wang, N. Raju, A. Epstein, L.-S. Tan, A. Urbas, L. Y. Chiang and B. Hu, *J. Am. Chem. Soc.*, 2012, **134**, 3549-3554.

[30] L. He, M. Li, A. Urbas and B. Hu, *Adv. Mater.*, 2014, **26**, 3956-3961.

[31] H. Xu, M. Wang, Z.-G. Yu, K. Wang and B. Hu, *Adv. Phys.*, 2019, **68**, 49-121.

[32] C. Grewer and H.-D. Brauer, *J Phys. Chem.*, 1994, **98**, 4230-4235.

[33] F. Wilkinson and A. A. Abdel-Shafi, *J. Phys. Chem. A*, 1999, **103**, 5425-5435.

[34] F. B. Dias, J. Santos, D. R. Graves, P. Data, R. S. Nobuyasu, M. A. Fox, A. S. Batsanov, T. Palmeira, M. N. Berberan-Santos and M. R. Bryce, *Adv. Sci.*, 2016, **3**, 1600080.

[35] M. K. Etherington, J. Gibson, H. F. Higginbotham, T. J. Penfold and A. P. Monkman, *Nat. Commun.*, 2016, **7**, 13680.

[36] J. Gibson, A. P. Monkman and T. J. Penfold, *ChemPhysChem*, 2016, **17**, 2956-2961.

[37] P. L. dos Santos, M. K. Etherington and A. P. Monkman, *J. Mater. Chem. C*, 2018, **6**, 4842-4853.

[38] R. S. Nobuyasu, Z. Ren, G. C. Griffiths, A. S. Batsanov, P. Data, S. Yan, A. P. Monkman, M. R. Bryce and F. B. Dias, *Adv. Opt. Mater.*, 2016, **4**, 597-607.

[39] T. J. Penfold, E. Gindensperger, C. Daniel and C. M. Marian, *Chem. Rev.*, 2018.

[40] L. Ouahab and T. Enoki, *Eur. J. Inorg. Chem.*, 2004, **2004**, 933-941.

[41] N. Hanasaki, H. Tajima, M. Matsuda, T. Naito and T. Inabe, *Phys. Rev. B*, 2000, **62**, 5839.

[42] C. Hintze, U. E. Steiner and M. Drescher, *ChemPhysChem*, 2017, **18**, 6-16.

[43] M. Li, L. He, H. Xu, M. Shao, J. Tisdale and B. Hu, *J. Phys. Chem. Lett.*, 2015, **6**, 4319-4325.
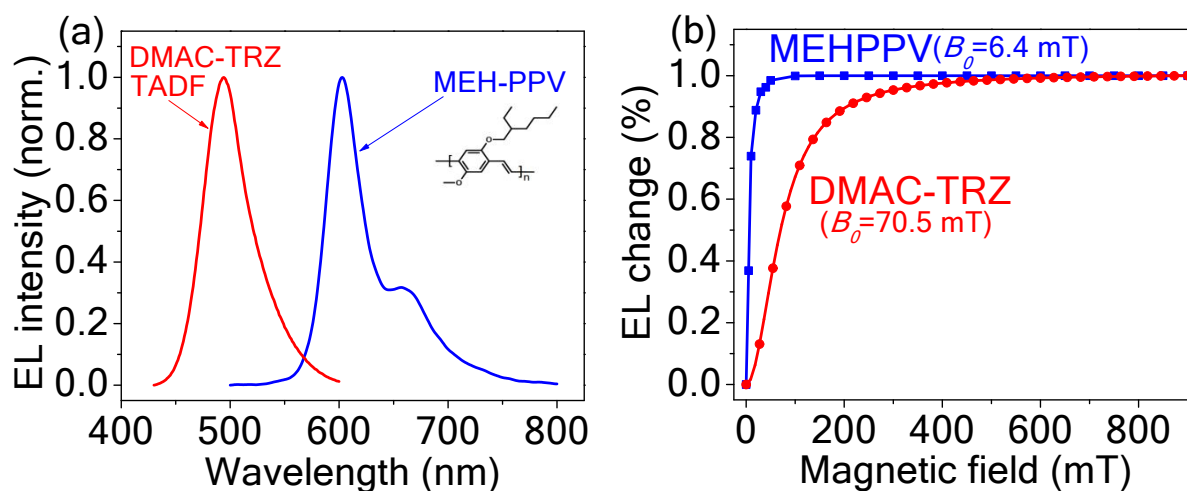
Figures

Figure 1. (a) EL spectra for MEH-PPV and DMAC-TRZ OLEDs. The OLED devices were fabricated with the structure of ITO/PEDOT:PSS/ active layer/B-phen/Al. (b) Magneto-EL occurring at hyperfine interaction regime (< 10 mT) in MEH-PPV and at spin-orbital coupling regime (> 10 mT) in DMAC-TRZ, shown as narrow and broad curve shapes. The internal magnetic parameter B_0 was fitted by using Lorentzian equation $MFE = \alpha\dfrac{B^2}{B^2 + B_0^2}$.
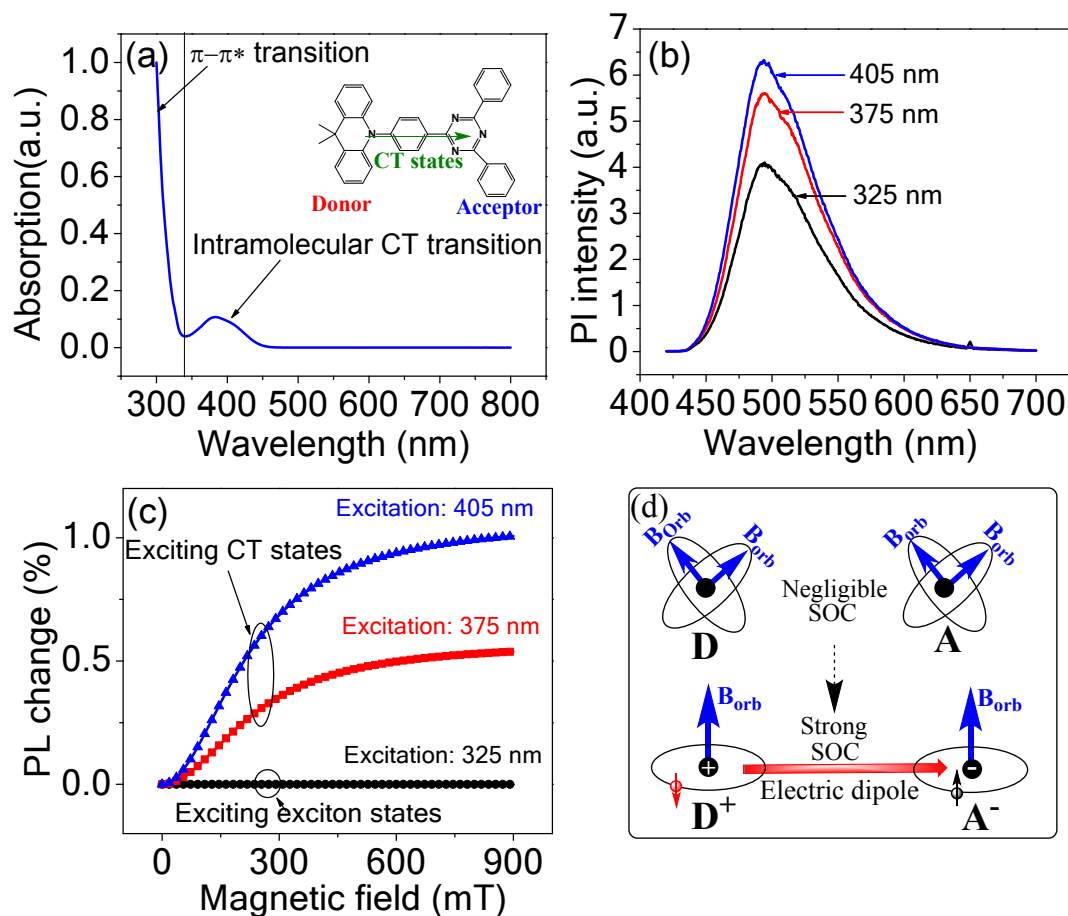
Figure 2. Excitation wavelength dependence of magneto-PL. (a) UV-Vis absorption spectrum of DMAC-TRZ in toluene solution. The inset shows the molecular structure of DMAC-TRZ with donor and acceptor moieties; (b) PL spectra and (c) magneto-PL for DMAC-TRZ in toluene solution under 325nm, 375nm and 405nm laser beam excitation; (d) SOC generated by polarizing orbitals due to electrical dipole between D^+ and A^- within a CT state.
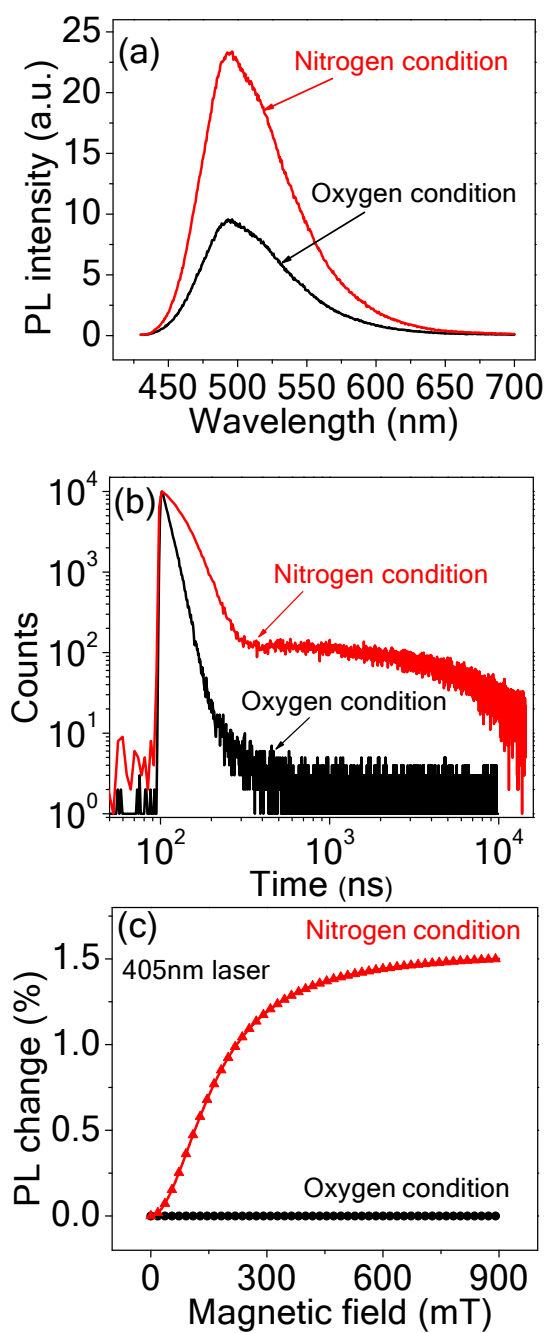
Figure 3. Characterization on DMAC-TRZ in toluene solutions separately applied with N_2 and O_2: (a) steady state PL spectra; (b) PL decay curves; (c) magneto-PL signals under 405 nm laser beam excitation with the intensity of 400 mW/cm^2.
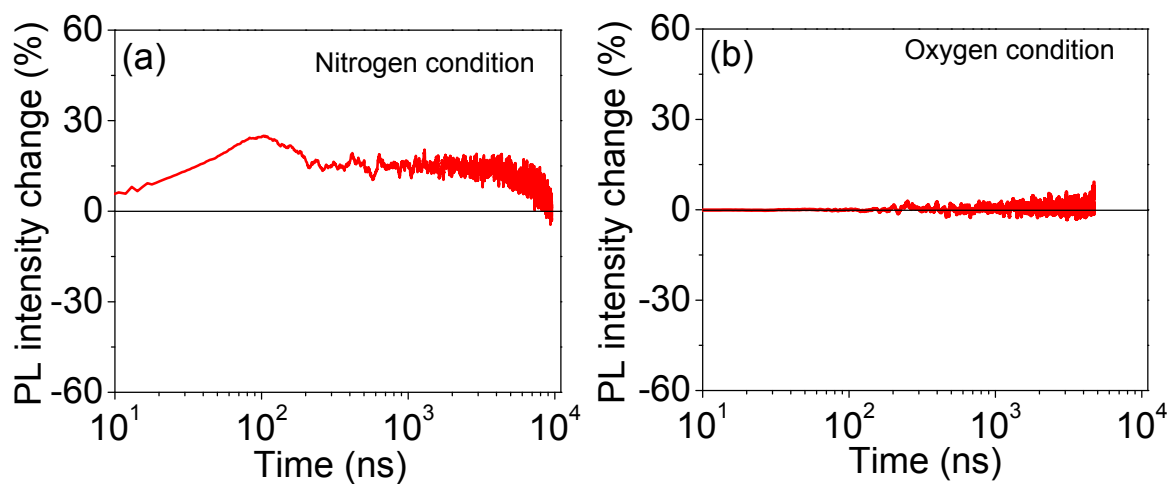
Figure 4. PL decay dynamics with magnetic field (200 mT) at SOC regime for DMAC-TRZ in toluene solution. The PL intensity change, defined as (PL $_{magnetic\ field}$ - PL $_{zero\ field}$)/ PL $_{zero\ field}$, is measured by comparing the PL decay curves in magnetic field (200mT) and zero field. (a) PL intensity change as the function of decay time under nitrogen condition. (b) PL intensity change as the function of decay time for oxygen condition. The magnetic field has negligible influence for PL decay dynamics under oxygen condition.
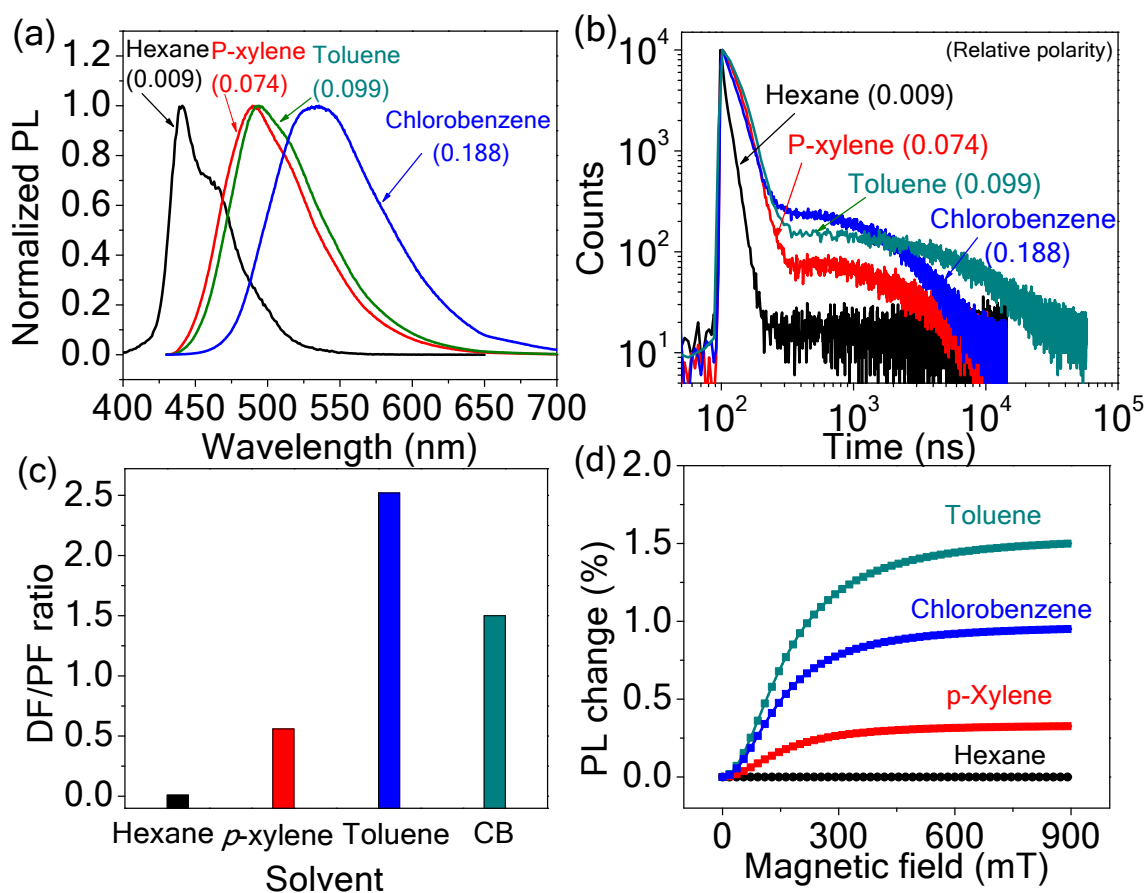
Figure 5. Characterization on DMAC-TRZ in solutions with four different solvents: Hexane (relative polarity 0.009), p-xylene (relative polarity 0.077), toluene (relative polarity 0.099), and chlorobenzene (CB) (relative polarity 0.188). The polarity of water is set to be unity. (a) Normalized PL spectra; (b) PL delay curves; (c) DF/PF ratio calculated from PL delay curves; (d) Magneto-PL for those DMAC-TRZ solutions under 405 nm laser excitation with the intensity of 400mW/cm^2.

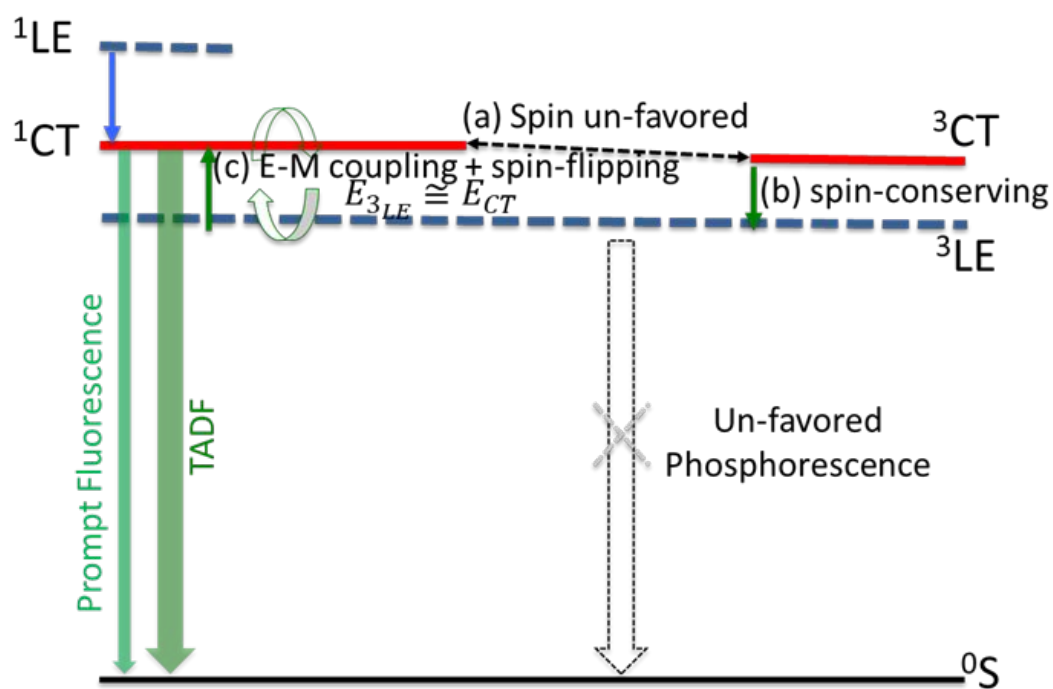Figure 6. The prompt fluorescence by the ^{1}LE-^{1}CT-^{0}S process (blue) and TADF based on the ^{3}LE-^{1}CT-^{0}S process (green), and proposed mechanism for transition between ^{1}CT, ^{3}CT and ^{3}LE states. In order to realize the efficient TADF through ^{3}LE -to-^{1}CT conversion, ^{3}LE state should have similar energy level with CT states ($E_{3_{LE}} \cong E_{CT}$). (a) The intersystem crossing between ^{3}CT to ^{1}CT is un-favored due to intramolecular exchange interaction. (b) Internal conversion from ^{3}CT to ^{3}LE is allowed through spin conservation, (c) Spin mixing from ^{3}LE state to ^{1}CT is critically required to generate TADF through endothermic process due to SOC-induced spin flipping under electric-magnetic (E-M) coupling between ^{1}CT and ^{3}LE. The un-favored exothermic transition from ^{3}LE to S_0 is suppressed by the E-M coupling between ^{3}LE and ^{1}CT to generate a low-efficiency phosphorescence.

ToC
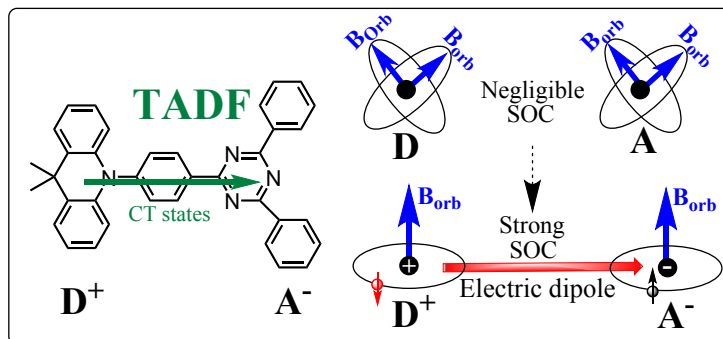
The spin-orbital coupling effects and underlying spin-dependent processes of enabling high-efficiency TADF is revealed based on the magneto-optical studies.